International Journal of Astrobiology 16 (2): 190–199 (2017)
doi:10.1017/S1473550416000173

Biochip-based instruments development for space exploration: influence of the antibody immobilization process on the biochip resistance to freeze-drying, temperature shifts and cosmic radiations

G. Coussot[1], T. Moreau*, C. Faye[2], F. Vigier*, M. Bagué[3], A. Le Postollec[4,5], S. Incerti[6], M. Dobrijevic[4,5] and O. Vandenabeele-Trambouze[7,8]

[1]*Institut des Biomolécules Max Mousseron-IBMM, Centre National de la Recherche Scientifique, Université de Montpellier, Unité Mixte de Recherche 5247, Faculté de Pharmacie, 34093 Montpellier cedex 5, France e-mail: gaelle.coussot@umontpellier.fr*
[2]*COLCOM, Cap Alpha, 34830 Clapiers, France*
[3]*German Aerospace Center (DLR), Institute of Planetary Research, Berlin, Germany*
[4]*Université de Bordeaux, LAB, UMR 5804, F-33270 Floirac, France*
[5]*CNRS, LAB, UMR 5804, F-33270 Floirac, France*
[6]*University of Bordeaux, CENBG, UMR 5797, F-33170 Gradignan, France*
[7]*Université de Bretagne Occidentale (UBO, UEB), IUEM–UMR 6197, Laboratoire de Microbiologie des Environnements Extrêmes (LMEE), Plouzané, France*
[8]*Ifremer, UMR6197, LMEE, Plouzané, France*

Abstract: Due to the diversity of antibody (Ab)-based biochips chemistries available and the little knowledge about biochips resistance to space constraints, immobilization of Abs on the surface of the biochips dedicated to Solar System exploration is challenging. In the present paper, we have developed ten different biochip models including covalent or affinity immobilization with full-length Abs or Ab fragments. Ab immobilizations were carried out in oriented/non-oriented manner using commercial activated surfaces with *N*-hydroxysuccinic ester (NHS-surfaces) or homemade surfaces using three generations of dendrimers (dendrigraft of poly L-lysine (DGL) surfaces). The performances of the Ab -based surfaces were cross-compared on the following criteria: (i) analytical performances (expressed by both the surface density of immobilized Abs and the amount of antigens initially captured by the surface) and (ii) resistance of surfaces to preparation procedure (freeze-drying, storage) or spatial constraints (irradiation and temperature shifts) encountered during a space mission. The latter results have been expressed as percentage of surface binding capacity losses (or percentage of remaining active Abs). The highest amount of captured antigen was achieved with Ab surfaces having full-length Abs and DGL-surfaces that have much higher surface densities than commercial NHS-surface. After freeze-drying process, thermal shift and storage sample exposition, we found that more than 80% of surface binding sites remained active in this case. In addition, the resistance of Ab surfaces to irradiation with particles such as electron, carbon ions or protons depends not only on the chemistries (covalent/affinity linkages) and strategies (oriented/non-oriented) used to construct the biochip, but also on the type, energy and fluence of incident particles. Our results clearly indicate that full-length Ab immobilization on NHS-surfaces and DGL-surfaces should be preferred for potential use in instruments for planetary exploration.

Received 26 September 2015, accepted 5 April 2016, first published online 28 June 2016

Key words: Astrobiology, biochip, search for Extraterrestrial Life, space constraints.

Introduction

Antibody (Ab) chips have a strong background not only in clinical and biomedical applications but also in the analysis of environmental contaminants as a result of small samples, reagent volume consumption and short assay time. In order to realize an assay, one of the important requirements is the immobilization of Abs on the material surface. Choosing the best Ab/material surface arrangement is challenging due to: (i) the huge diversity of materials (glass, polystyrene (PS), polypropylene, etc.) commercially available, (ii) the wide range of immobilization processes and chemistries that can be chosen (adsorption, covalent linkage, oriented immobilization through affinity partner) and (iii) the possibility to use whole Ab (usually IgG) or Ab fragments, such as Fab and $F(ab')_2$ (Angenendt 2005; Jonkheijm *et al.* 2008; Batalla *et al.* 2009; Kozak *et al.* 2009).

Over the last few years, Ab chips have been recommended by space agencies for Solar System exploration. Considering their

* These authors are now working in private companies.

size and weight (miniaturized system), the number of analyses that can be performed simultaneously and the number of targets that can be addressed, these biochips are promising tools for the search for clues of extinct or extant life. Several biochip-based instruments are under development for space exploration (Le Postollec *et al.* 2007; Parro *et al.* 2008; Martins 2011; Parro *et al.* 2011, Sims *et al.* 2012; McKay *et al.* 2013), but few data are available in the literature on the ability of Ab chips to resist space constraints such as irradiation, thermal shifts or freeze-drying. Recently, studies have demonstrated that cryoprotectants or thermal protectants help in stabilizing Ab chips for long-time storage, temperature shifts or freeze-drying (Wang *et al.* 2007; Baqué *et al.* 2011; de Diego-Castilla *et al.* 2011). Regarding the resistance to cosmic rays, the type of particles that a biochip can face in space has been defined (Le Postollec *et al.* 2009a) and the influence of several particles on Ab has been studied (Le Postollec *et al.* 2009b; Baqué *et al.* 2011, 2015; de Diego-Castilla *et al.* 2011). These previous results suggest that the close environment (ions, storage additives) of Abs greatly influences its resistance to space constraints. Nevertheless, the influence of the biochip model (mainly the way used to immobilize the Ab to the surface of the chip) on the Ab resistance to space constraints has never been evaluated. It has been shown that the Ab immobilization processes used to develop devices for biomedical applications influence their analytical properties (Butler 2000; Batalla *et al.* 2008). So, in the present paper, we have tested various Ab immobilization processes in order to study the resistance of immobilized Ab to cosmic rays. Indeed, high reactivity and binding capacity of Ab is crucial for the use of biochip-based instruments especially when target compounds are present at trace levels like in extraterrestrial matter. In this context, we studied the grafting of full-length Ab and Ab fragments on various material chip surfaces with different buffers. In particular, we studied oriented or random immobilization, covalent or affinity linkage and two different interfaces (protein A/G or dendrimer). Considering the long duration of space mission (several years), only covalent and affinity immobilization were selected. Immobilization by Ab adsorption was not studied here because it is known that adsorbed Ab can be easily denatured by the contact with the chip surface, which induces important Ab binding capacity losses (Butler 2004). Anti-horseradish peroxidase (HRP) Ab was utilized as a model Ab since the HRP/anti-HRP binding has been already investigated to study immobilization protocol and surface functionality (Fuentes *et al.* 2006; Batalla *et al.* 2008; Dixit & Kaushik 2012).

The resistance of various Ab surfaces, for various irradiation experiments (including neutron, proton, electron and carbon ion) will be described in parallel with the comparison of analytical performances of the surfaces. Studies were done using PS microwell format as described in Baqué *et al.* (2011) because polymeric materials are easily functionalized and present interesting mechanical resistance. The amount of immobilized Ab and the binding capacity of immobilized Ab will be estimated using Amino Density Estimation by Colorimetric Assay (ADECA) and Antibody Anti-HorseRadish Peroxidase (A_2HRP) methods, respectively (Coussot *et al.* 2011a, b, Moreau *et al.* 2011). In addition, resistance to surface preparation procedure or other spatial constraints (freeze-drying, storage and temperature shifts) will be summarized in the last section.

Material and methods

Chemical, reagents and materials

Mouse monoclonal anti-HRP Abs were obtained from MyBioSource (clone number B215M, USA). DNA Bind Stripwell Plates containing *N*-hydroxysuccinimide modified surface (referred as *N*-hydroxysuccinic ester (NHS) surfaces), sodium azide, BSA (bovine serum albumin for biochemistry, fraction V, 96–100% protein), Tween® 20, glutaraldehyde solution (grade II, 25%), sodium acetate trihydrate, *o*-phenylenediamine dihydrochloride (OPD-2HCl), hydrogen peroxide (H_2O_2) solution 30% (w/w) in water and sodium borohydride ($NaBH_4$) were obtained from Sigma Aldrich (France). Dendrigraft of poly L-lysine (DGL, generations G2, G3, G4), *N*-gamma-maleimidobutyryl-oxysuccinimide ester (GMBS, referred as NHS-maleimide linker in the following section) and Coomassie Brilliant Blue G-250 (CBB) were provided by Colcom (France, http://www.colcom.eu) and used as received. Protein A/G coated stripwell plates, Slide-A-Lyzer devices, 10 K MWCO, Superblock buffer™ and reducing agent Tris (2-carboxyethyl)-Phosphine Hydrochloride (TCEP.HCl) were obtained from Thermo Fisher Scientific (France). Phosphate-buffered saline (PBS) was obtained from Euromedex (France) (10× solution, pH 7.4, 10 mM, used in a final concentration of 1× in water solvent). The ultra-pure water was obtained from a Millipore Purification system. Other chemicals are analytical grade and used as received.

Ab and fragment immobilization process

Ab fragments preparation

Fab and F(ab′)$_2$ fragments are prepared and characterized using the procedure described previously (Faye *et al.* 2012). Fab′ fragments are obtained by reduction of F(ab′)$_2$ using TCEP–HCl as the reducing agent: TCEP–HCl (5 mM) is added to the F(ab′)$_2$ solution and left for 5 min at room temperature (RT). The reducing agent is then removed with dialysis of the Fab′ sample against PBS for at least 1 h.

Covalent full-length Ab and Fab/F(ab′)$_2$ fragments immobilization on NHS surfaces

The Ab immobilization protocol was adapted from Baqué *et al.* (2011) protocol using 200 µg ml^{-1} of full-length Ab, Fab and F(ab′)$_2$ solutions in a PBS buffer containing 0.05–0.09% sodium azide and on microwells functionalized with NHS ester end groups (DNA-Bind™). After immobilization, to prevent non-specific binding, a saturation step with BSA solution (3% (w/v) in PBS) was carried out (Baqué *et al.* 2011) followed by washings with PBS buffer containing 0.05% Tween® 20 (PBST) and then with PBS. This direct and covalent

https://doi.org/10.1017/S1473550416000173 Published online by Cambridge University Press

approach onto NHS surface resulted in non-oriented immobilization of Ab and its fragments.

Covalent full-length Ab and Fab/F(ab′)$_2$ fragments immobilization on DGL interfaces

We introduced aminated dendritic interfacing layer called DGL. DGL are synthesized using an iterative process (Collet *et al.* 2010). The main characteristics of DGL are the following: (i) they are fully soluble in water (Collet *et al.* 2010; Romestand *et al.* 2010), (ii) they are non-toxic (Romestand *et al.* 2010), (iii) they are non-immunogenic (Romestand *et al.* 2010), (iv) they have a high number of amine groups (lysine) on their surface for subsequent grafting (Collet *et al.* 2010; Coussot *et al.* 2011b), (v) they can be grafted as a monolayer using various chemistry (Coussot *et al.* 2011b), and (vi) they are highly stable under high temperature including sterilization conditions (Commeyras *et al.* 2006). The DGL surfaces have been prepared using a protocol adapted from Coussot *et al.* (2011a). Briefly, DGL grafting was performed on microwells functionalized with NHS ester end groups, using 250 µl of DGL solutions (DGL-G2, DGL-G3 or DGL-G4) at 2 mg ml^{-1} in a carbonate-bicarbonate buffer (0.1 M, pH 9.4) and left for 2 h at RT under agitation using a microplate agitator (450 rpm). The resulting DGL-coated microwells were placed in a methanol-carbonate buffer bath (50/50: v/v) (MeOH: 250 mM carbonate-bicarbonate buffer, pH 11.25) in an ultrasonic container for 1 h at RT in order to remove non-covalently linked DGL. The DGL-coated wells were then rinsed with ultra-pure water before activation step with bifunctional linker glutaraldehyde.

For full-length Ab immobilization, DGL-coated wells were activated using 250 µl of a 12.5% (v/v) glutaraldehyde solution in sodium acetate buffer (3 M, pH 8) and left for 1 h at RT under gentle agitation. Activated DGL-coated wells were then washed three times with PBS. Immediately, after washing step, activated DGL-coated wells were filled with 100 µl of full-length Ab at 200 µg ml^{-1} in PBS containing azide and incubated at RT for 20 min. Then microwells were saturated for 10 min (see NHS protocol) and filled with 250 µl of $NaBH_4$ at 10 mg ml^{-1} in ultra-pure water, incubated at RT for 30 min, in order to reduce all glutaraldehyde functions (named G) that remain available. The resulting Ab–G–DGL–NHS surface was finally washed three times with PBST and twice with PBS. Consequently, the full-length Abs have been coupled randomly to the DGL interface.

For Fab/F(ab′)$_2$ fragment immobilization, DGL-coated wells were activated using 100 µl of an NHS-maleimide linker solution, which was prepared at 200 µg ml^{-1} in a DMSO–PBS buffer (1/9:v/v), with PBS adjusted to pH 8 for site-directed oriented immobilization of Ab fragments. The activated DGL-coated wells were left for 1 h at RT under gentle agitation. The resulting Fab (or F(ab′)$_2$)–maleimide–DGL–NHS surface were then washed three times with PBS. Immediately after the washing step, fragments diluted in PBS were added and surface was saturated with BSA solution (3% (w/v) in PBS) followed by washing steps as described previously with Ab or Fab/F(ab′)$_2$ direct immobilization on NHS surface.

Oriented immobilization of full-length Abs using protein A/G

Commercially available plates uniformly and stably coated with protein A/G were used to directly capture full-length Ab. The protein A/G-coated wells were washed three times with PBST prior to use them. Immobilization was performed with 100 µl of full-length Abs at 10 µg ml^{-1} in blocking buffer (Superblock®), for 2 h at RT under gentle agitation. The resulting Ab-protein A/G-coated surface was washed once with PBS then followed by a saturation step with 250 µl of Superblock® buffer, with a minimum incubation time of 30 min at RT under agitation. Washing steps were carried out with PBS and PBST as described previously.

Irradiation experiments

The irradiation effects are evaluated using A_2HRP method (described in section 'Sample freeze drying, temperature shift cycles and sample storage'), by comparing the results of irradiated samples to those of non-irradiated controls. Particle types and energy were defined considering the particles a biochip would face during interplanetary travel (Le Postollec *et al.* 2009a; McKenna-Lawlor *et al.* 2012). As the composition of Galactic Cosmic rays (GCRs) is roughly 85–90% protons, 10–13% helium, about 1% electrons and about 1% heavier nuclei (O'Neill 2010), we chose to perform protons, electrons and carbon ions irradiations. Approximately 9 MeV electrons, 62 MeV nuc^{-1} carbon ion and 15–30 MeV protons effects were tested on prepared Ab surfaces. We also decided to perform neutron experiments, as neutrons are abundant on Mars' surface due to particles interactions with Mars's atmosphere and regolith (Hassler *et al.* 2012; Köhler *et al.* 2014). Controls were prepared with the same immobilization procedure and conditioning, and were transported in the same conditions than irradiated samples but were not exposed to particles radiations.

Neutron and proton irradiation

Neutron and proton irradiations had already been performed at low energy (few MeV) and described in previous work (Le Postollec *et al.* 2009b; Baqué *et al.* 2011). The irradiations considered here were performed at higher energies at the cyclotron of Louvain-la-Neuve. The mean energy of neutrons was 16.56 MeV and samples were positioned, so that there received two different fluences (3×10^{12} and 3×10^{13} neutrons cm^{-2}). For protons, five different energies (14.4, 20.9, 25.9, 29.4 and 50.5 MeV) and two fluences (3×10^{11} and 3×10^{12} protons cm^{-2}) were used. All the parameters are described in detail in Baqué *et al.* (2015).

Electron irradiation

The electron irradiation is described in Baqué *et al.* (2015). It was performed at the *Institut Bergonié* (Bordeaux, France). The samples received 9 MeV electrons during 7 and 70 min corresponding respectively to 1400 MU (Monitor Unit) and 14 000 MU, i.e. 2.3×10^{10} and 2.3×10^{11} electrons cm^{-2}, according to Gobet *et al.* (2015). Samples were irradiated in their conditioning bag (lyophilized form).

https://doi.org/10.1017/S1473550416000173 Published online by Cambridge University Press

Carbon ion irradiation

The ^{12}C irradiation parameters are described in Baqué *et al.* (2015). The irradiation was performed at the *Laboratori Nazionali del Sud* of the *Instituto Nazionale di Fisica Nucleare* (Catana, Italy). Samples were irradiated with 62 MeV nuc^{-1} ^{12}C particles with a target fluence of 2.16×10^6 particles cm^{-2} which corresponds, considering CREME96 data, to the fluence expected for 18 months at 1 AU (Astronomical Unit). Samples were irradiated in their conditioning bag (lyophilized form).

Sample freeze drying, temperature shift cycles and sample storage

Sample freeze drying – Samples were freeze-dried according to the procedure of Baqué *et al.* (2011) with the following conditions: 120 µl of the sugar-containing freeze drying buffer were added to each well after the saturation step. Then the samples were frozen with liquid nitrogen and placed within a home-made aluminium case before transferring them into the freeze-dryer (Christ Alpha 2–4). Freeze-drying was performed overnight at −85°C and 0.05 mbar. When freeze-drying process was achieved, the chamber of the freeze-dryer was filled with nitrogen gas to limit the contact with humidity-charged air. The sample-containing aluminium case was then sealed. The sealed aluminium case was then transferred in a glove box (Ateliers de Technochimie, Ivry sur Seine, France) preconditioned with inert gas (Argon, Linde). After opening the aluminium case, freeze-dried samples were either immediately analysed or put under vacuum into plastics bags and stored at 4°C before irradiation or temperature shift tests. Non-lyophilized controls followed the whole preparation process except for freeze-drying step.

Temperature shifts – Samples from the same freeze-drying batch were selected and divided into two groups: one group was exposed to five cycles ranging from −10 to +44°C at 0.3°C min^{-1} and the other group stayed at +4°C (temperature shifts controls).

Storage – Samples from the same freeze-drying batch were selected and divided into different plastic bags so that only one series of samples could be rehydrated at a time, the other bags being stored at 4°C. Results of the stored samples were compared with those obtained immediately after preparation.

All the binding surface capacities were evaluated both: (i) just after their preparation and (ii) after the exposure to space constraints using the A_2HRP method (see subsection 'A_2HRP method for estimating binding capacity of immobilized Abs').

Analytical procedures

ADECA method for estimating the total amount of immobilized Abs

ADECA allows calculating the total amount of grafted dendrimers or anti-HRP Abs (active plus non-active) whatever the shape and composition of the surface (Coussot *et al.* 2011a, b; Moreau *et al.* 2011). ADECA was performed as described previously using CBB reagent (Coussot *et al.* 2011a, b; Moreau *et al.* 2011). The released acidified CBB was recorded at 610 nm with an Infinite 200™ absorbance microplate reader from Tecan having a wide measurement range up to 3.6 absorbance unit.

For NHS surfaces, ADECA was performed before BSA saturation. The measured absorbance of the solution after washing (ADECA blank) was statistically identical from that of background measured on the native NHS surface suggesting no CBB non-specific binding to the NHS surface.

For DGL surfaces, ADECA was performed three times: firstly after NHS surface coating (DGL grafting), secondly after surface activation (addition of linkers onto DGL-surface) and finally after Ab or fragment grafting. We checked that ADECA blank values were not significantly different from those obtained with wells containing no DGL (raw NHS surface). After Ab or fragment immobilization, blank values were compared with blanks from DGL surfaces. For all biochip models, $n = 4$–10 replicates were done, depending on the quantity of samples available.

A_2HRP method for estimating binding capacity of immobilized Abs

A_2HRP method provides a measure of the amount of active anti-HRP Abs (Moreau *et al.* 2011). When combined to ADECA, the A_2HRP method permits the surface Ab-specific activity determination expressed in per cent. The A_2HRP method is based on HRP recognition by immobilized Ab. In addition, in the presence of H_2O_2 and OPD (chromogenic compound), HRP catalyses a reaction to form mainly brown colour 2, 3 DiAminoPhenazine (DAP) product, this coloured products was detected at 490 nm with an absorbance microplate reader from Tecan Company. A_2HRP was performed as described previously (Moreau *et al.* 2011) on saturated BSA Ab surfaces. A_2HRP was used to evaluate surface performances and Ab resistance after: (i) exposure to irradiations, (ii) storage, (iii) freeze-drying procedure and (iv) temperature shifts. For freeze-dried samples, a rehydration step was done prior to analysis. Blanks for A_2HRP method were performed using wells that did not contain Ab nor Ab fragment (in other words, NHS surface, protein A/G surface or DGL surface with linker).

Statistical treatment

Irradiation effects were evaluated by comparing the mean signal values obtained for non-irradiated controls and for irradiated samples. Thus, Student's *t*-tests were used to compare irradiated samples distribution and references distribution, taking into account the number of repetitions and the standard deviation (SD) of each distribution. The differences between these two distributions were considered statistically significant with a 95% level of confidence when the calculated *P*-values were below the 0.05 threshold value.

Results and discussion

Ab surfaces: immobilization step and surface densities

A large diversity of chemistries have been developed to generate protein biochips (Jonkheijm *et al.* 2008) leading to various

https://doi.org/10.1017/S1473550416000173 Published online by Cambridge University Press

surface types and performances (Angenendt 2005). In this paper, both commercial and homemade chemistries were studied: ten different models of Ab biochips, involving random and oriented Ab immobilization using covalent chemistry or affinity interactions. Full-length Ab or Fab/F(ab′)$_2$ fragments were also bound to an interfacing layer covalently grafted on NHS surfaces. We chose aminated dendritic interfacing layer called DGL. Thanks to the tridimensional structure of DGL, this interfacing layer will contribute to distance Abs from PS surfaces thus preserving them from denaturation (Qian *et al.* 2000; Jung *et al.* 2008).

In the present paper, we studied three generations of DGL (DGL-G2, DGL-G3 and DGL-G4) layers, which were covalently bound on PS material. Representation of studied Ab surfaces and their relative costs are reported in Table 1. ADECA method was used to control all grafting steps in surface preparation and to calculate the initial density of immobilized Ab. Estimation of the density of immobilized Ab provides crucial information that permits to define the flux of particles required during irradiation. Indeed, a sufficient proportion of Abs should be irradiated to evaluate the conservation of the binding capacity of the surface (see irradiation in subsection 'Resistance of Ab-based surfaces to irradiation').

Multiple steps are required to develop a chip assay including chemical/affinity reactions with material and/or proteins. ADECA was used throughout the immobilization phases to control the quality of each step. As an example, results obtained with full-length Ab on NHS and DGL-G3 surfaces are reported in Fig. 1. As previously shown, DGL lead to stable monolayer surfaces with a higher number of amines as commercial surfaces (Coussot *et al.* 2011b). The amount of immobilized full-length Ab was evaluated to be 5.6×10^{11} (0.90 ± 0.04 N$^+$ nm^{-2}) and up to 8.5×10^{11} (3.00 ± 0.02 N$^+$ nm^{-2}) on NHS or DGL surfaces, respectively. These Ab surface densities are in accordance with those previously obtained on NHS surfaces (Moreau *et al.* 2011) or using PAMAM dendrimers (Trévisiol *et al.* 2003).

After reacting the NHS surface group with DGL interfacing layer, the relatively stable but highly reactive maleimide group allows the coupling of the Fab/F(ab′)$_2$ fragments in an oriented manner. Experimental conditions were fixed at pH 7.4 to control immobilization process by avoiding random immobilization resulting from non-specific reactions of the maleimide group with amine, which can occur with pH above 9 (Liu *et al.* 2000; Rusmini *et al.* 2007). For all Fab (or F(ab′)$_2$)-maleimide-DGL(G2, G3, G4)-NHS surfaces, amine density was about 0.50 N$^+$ nm^{-2} (RSD < 7%), whereas NHS-surfaces gave twice more N$^+$/nm^2 with random immobilization: 1.10 N$^+$ nm^{-2} (RSD: 2.2%) for Fab-NHS surfaces and 1.20 N$^+$ nm^{-2} (RSD: 1.6%) for F(ab′)$_2$-NHS surfaces. As expected, our results also demonstrate that maleimide chemistry leads to a lower surface coverage than the glutaraldehyde one or than direct coupling to NHS surfaces (Peluso *et al.* 2003).

ADECA was not performed for protein A/G surface, because of its coating instability under ADECA conditions (Coussot *et al.* 2011b).

Table 1. *Listing of chemistries used for Ab immobilization onto PS material with/without DGL interface and space-related parameters (irradiation, freeze-drying, storage and thermal shifts) evaluated for each Ab surfaces type*

	NHS-surface				DGL (G2, G3, G4) surface			Protein A/G surface
	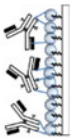							
Chemical reactive group for Ab grafting	Ester *N*-hydroxysuccinic (NHS)				Glutaraldehyde with $NaBH_4$ reduction (G)	Maleimide	/	
Immobilization	Covalent random				Covalent random	Covalent oriented	Affinity oriented	
AAb type	Full-length	Fab	F(ab')$_2$		Full-length	Fab′	Full length	
Antibody consumption (mg)	1.2	1.3	3		1.2	3	0.1	
Total cost (€) per microplate	174	182[a]	414[a]		274[b]	511[ab]	48	
Irradiations experiments	X	X	X		X (DGL-G2; DGL-G3)	ND	X	
Freeze-drying	X	X	X		X (DGL-G3)	X (DGL-G3)	X	
Storage	X	ND	ND		X	X (DGL-G3)	X	
Thermal shifts	X	X	X		X (DGL-G3)	ND	X	

Total cost includes microplates and reagents (functional linkers, Abs and DGL), but does not include the buffer cost (used for all chemistries) nor manpower. To be able to compare costs between experiments and Ab types, the Ab consumption was calculated for the theoretical preparation of one microplate (96-wells) with the knowing that under our experimental conditions.
[a]95% of full-length Abs were able to be converted into Fab fragments but only 40% for F(ab')$_2$ fragments.
[b]Cost of DGL G3 was considered here (intermediate price between G2 and G4).
ND, not determined.

https://doi.org/10.1017/S1473550416000173 Published online by Cambridge University Press

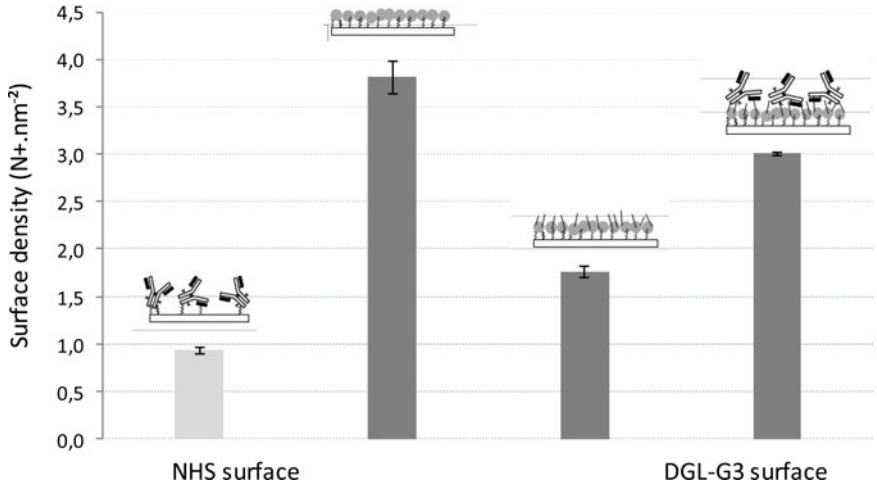

Fig. 1. ADECA results expressed in amines (N^+) per nm^2 for the study of Ab immobilization on commercially available NHS surface (pale grey) and homemade DGL–G3 surface (dark grey). For the building of DGL–G3 surfaces, three ADECA controls were required. After step 1, ADECA permits to evaluate the number of available amines of DGL bound to NHS surface. After step 2 (activated DGL–G3 surface): ADECA allows us to quantify the amines that did not react with the glutaraldehyde linker (proof of activation). After step 3, ADECA estimate all the available amino groups present on the Ab–G–DGL–NHS surface. Net absorbance values were calculated by subtracting the corresponding mean blank values to read samples values. The error bars represent a SD calculated with five replicates.

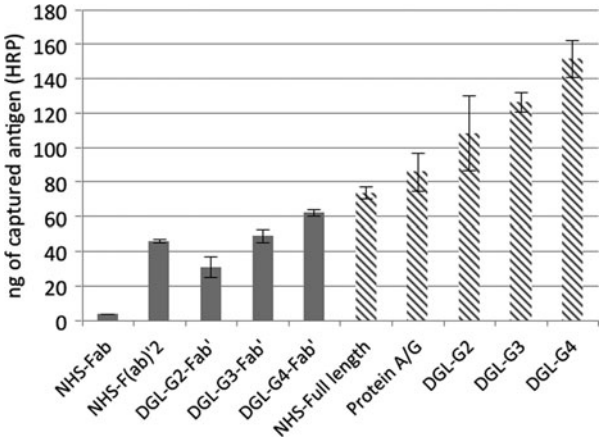

Fig. 2. Amount of HRP (in ng) captured by prepared Ab surfaces using Fab/F(ab′)$_2$ fragments (grey bars) or full-length Ab (hatched bars). Error bars correspond to a SD calculated with $n = 10$ assays for full-length Ab (five replicates done twice) or calculated with $n = 5$ repetitions for Fab/F(ab′)$_2$ fragments.

Binding capacity differences for full-length Abs or Fab/F(ab′)$_2$ fragments on NHS–protein A/G–DGL surfaces

Combined together, ADECA and A_2HRP methods allow the estimation of active Ab (or fragment) on a surface thanks to the knowledge of Ab surface density and the quantitation of captured antigen (HRP) (Coussot *et al.* 2011a, b; Moreau *et al.* 2011; Faye *et al.* 2012). In the present paper, we compared the binding capacities of the prepared Ab-based surfaces illustrated in Table 1. Discrepancy in the capacity of binding HRP antigen were observed between full-length Ab and Fab/F(ab′)$_2$ fragments (Fig. 2). Whatever the immobilization process used (random or oriented), the highest amount of captured HRP was observed using full-length Ab. This higher amount of captured antigens using full-length Ab surfaces was not due to a difference in their relative recognition properties. Indeed, the recognition property of fragments and full-length Ab were measured in solution. Results were statistically similar for all samples indicating that differences observed after immobilization are mostly due to the immobilization process (Faye *et al.* 2012). On commercial NHS-surface, only random immobilizations were performed. Our results show that the amount of antigens captured by the NHS-surface increases when increasing the protein size (Fab < F(ab′)$_2$ < full-length Ab). These results suggest that this can be due either to: (i) a reduced amount of immobilized fragments compared with full-length Ab (Peluso *et al.* 2003) or (ii) higher folding losses suffered by Fab/F(ab′)$_2$ fragments than by full-length Ab (Wängler *et al.* 2008; Moreau *et al.* 2011). The first hypothesis is not verified since amine densities were found to be 0.90 N^+ nm^{-2} for full-length Ab and 1.10 and 1.20 N^+ nm^{-2} for both Ab fragments suggesting higher ratio of fragment bound to NHS-surfaces (see above). We calculated that 56 ± 9% of NHS surface-immobilized full-length Ab still bind antigen. This result is in accordance with Moreau *et al.* (2011).

Comparing now the effects of oriented and non-oriented immobilization on antigen capture on DGL-interfaces, we can see that the amount of captured HRP with full-length Ab is about two or three times higher than with Fab′ immobilization with maleimide linker (Fig. 2). For both full-length Ab and Fab/F(ab′) fragments, we observed that (i) increasing the dendrimer generation (G2 → G3 → G4) increases the amount of captured HRP as previously suggested (Dixit & Kaushik 2012) and (ii) the amount of captured antigens seems to be correlated to the hydrodynamic radius of DGL (Moreau *et al.* 2011). Thus, the DGL-G4 leads to the greater amount of captured antigens (Fig 2). After grafting, above 70% of full-length Ab were active on DGL surfaces (whatever the DGL

https://doi.org/10.1017/S1473550416000173 Published online by Cambridge University Press

generation). These results are in agreement with the known properties of dendrimer interfaces that were developed to stabilize Ab surfaces and to increase the accessibility of binding sites to antigens (Singh *et al.* 1994; Trévisiol *et al.* 2003). These results clearly demonstrate that DGL-G4 allows efficient Ab immobilization. Oriented immobilization of full-length Ab with protein A/G surface leads to intermediate values of antigen binding ratios: a little bit higher than NHS surface but with a ratio lower than those obtained with all DGL surfaces. This result can probably be dependent on initial protein A/G density on PS material but we were not able to check this hypothesis due to the poor stability of the protein A/G layer under ADECA method.

These data demonstrated the influence of Ab surfaces type on its binding capacity. We were able to determine the antigen capture ability (optimum of binding) of each studied Ab surface. Per cent of active Abs has been calculated with the control (non-irradiated sample) values as being 100%. If Ab degradation occurred during irradiation experiments or transportation, then these values decreased.

To conclude, full-length Ab surfaces are easier to handle, less expensive (see Table 1) with higher binding antigen capacities. Consequently, we can assume that surfaces involving full-length Ab are more suitable for space applications (surfaces can face more damages without changing the analytical performance of the biochip, and the detection limit is better (we would be able to quantify fewer quantities of active Ab)).

Resistance of Ab-based surfaces to irradiation

The influence of Ab surface type on Ab stability under cosmic radiation is not known and must be studied before conducting exobiology experiments using biochips. Indeed, it has been shown that the physico-chemical environment of Ab influenced its resistance to irradiation since the buffer used for storage influences the Ab stability under gamma radiation (de Diego-Castilla *et al.* 2011). In order to evaluate if the Ab chip model influences Ab resistance under cosmic radiations, the amount of particles used during irradiation experiments were fixed, so that 41% of Abs received at least one proton (Coussot 2011a, b; Moreau 2011). Samples were irradiated using a fluence of about one particle per Ab molecule, which corresponds roughly to 10^3 times the fluence expected for a mission to Mars. Using such irradiation conditions, we measured from 12% to more than 95% surface binding capacities losses.

Our results demonstrated that 9 MeV electron and 62 MeV nuc^{-1} carbon ion irradiations do not significantly affect immobilized Ab and immobilized Ab fragments with the low (F_L) and high (F_H) fluences used. Neutron irradiations were performed only on full-length Ab grafted on NHS-surface and no significant degradation was detected. In Table 2, results are given as percentages of active Ab (± SD) that were normalized using the non-irradiated controls set at 100% (±10%). Values are only given when the activity of irradiated samples are significantly different (Student's *t*-test) to that of non-irradiated controls. Otherwise, non-significant effect (NSE)

Table 2. *Effect of irradiations expressed in % of active Abs on full-length Ab and Fab/F(ab')$_2$ fragments surfaces for various energies and fluences F_L and F_H used. ND indicates that no experiment was performed for these samples. NSE refers to non-significant effect*

			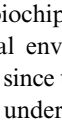		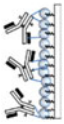					
	NHS-Full-length Ab		NHS-Fab		NHS-F(ab')$_2$		DGL-full-length Ab[a]		Protein A/G-full-length Ab	
Irradiation conditions	F_L	F_H	F_L	F_H	F_L	F_H	F_L	F_H	F_L	F_H
Protons 25 MeV[b]	81 ± 10	67 ± 14	60 ± 17[c,d]		69 ± 10[c,d]		NSE	54 ± 13		ND[e]
Electrons 9 MeV[g]	NSE	NSE	NSE	NSE	NSE	NSE	NSE	NSE		ND
Carbon ions 62 MeV nuc^{-1}[e]	NSE		ND		NSE		NSE			NSE

[a]Experiments were performed using DGL-G2 (Cyclotron Louvain-la-Neuve, Protons 25 MeV), DGL-G3 (Institut Bergonié, electrons 9 MeV) or DGL-G2, -G3 and -G4 (Instituto Nazionale di Fisica Nucleare, Carbon ions 62 MeV).
[b]$F_L = 3 \times 10^{11}$ protons cm^{-2} and $F_H = 3.10^{12}$ protons cm^{-2}.
[c]Mean of two different irradiation campaigns with $n = 5$ repetitions. Student's *t*-test indicates that the percentage of active Ab at F_L is equal to that at F_H.
[d]The mean percentage of active Ab was calculated using results obtained at both fluences.
[e]Experiments were not performed using 25 MeV but at 15–20 and 30 MeV (see Fig. 3).
[f]$F_L = 3 \times 10^{10}$ electrons and $F_H = 3 \times 10^{11}$ electrons.
[g]Only one fluence was applied for carbon ions.

https://doi.org/10.1017/S1473550416000173 Published online by Cambridge University Press

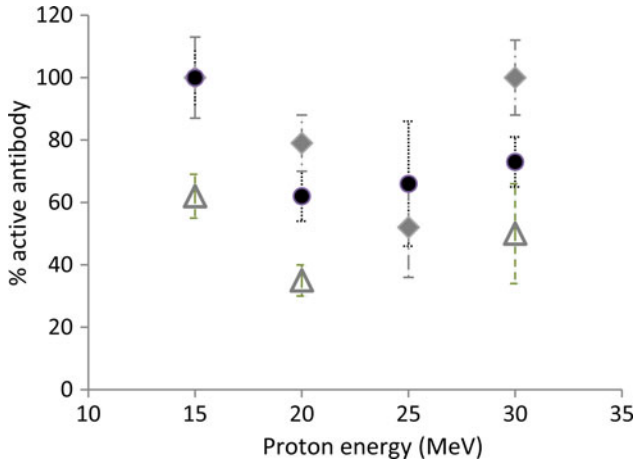

Fig. 3. Percentage of active Ab after proton irradiations at high fluences and energy ranging from 15 to 30 MeV for three different Ab surfaces (see Table 1): full-length Ab–NHS surface (grey quadrangle), full-length Ab–DGL–G3 surface (dark circle) and full-length Ab-protein A/G surface (empty triangle).

indicates that irradiated samples are significantly identical to their controls at 95% confidence level.

On the contrary, we observed that protons irradiation over the range 15–30 MeV can alter the whole Ab surface with a maximum loss in surface binding capacities for incident protons about 20–25 MeV (Fig. 3 and Table 2). For protein A/G surface (Fig. 3, 15–20–30 MeV protons energy), the loss in surface binding capacity might be due to a removal of the Ab from the surface (breaking either protein A/G/Ab interaction or PS material/protein A/G linkage) or to a loss of Ab recognition ability. Using Surface Plasmon Resonance, we demonstrated that no removal of immobilized Ab occurred (data not shown) thus decrease in binding capacities was only due to a loss of Ab recognition ability. Even if a degradation up to 65% of Ab (corresponding to 35% of surface active Ab) was measured for full-length Ab linked to protein A/G surface, Ab surfaces prepared exclusively with full-length Ab and without protein A/G have proven their ability to be used for planetary exploration. On the opposite, Fab/F(ab′)$_2$ fragment NHS-surface seems to be less sensitive to different fluences with relatively constant binding losses. There are more active Ab when combining both (i) full-length Ab–NHS surfaces and (ii) irradiation above 25 MeV under high fluence. This result suggests that this chip surface could be proposed in the development of future instrument to analyse organic matter in space. During the experiments using 25 MeV protons irradiation, we also demonstrated that the additional blocking step with BSA solution (see experimental section) helps to stabilize proteins during irradiations (7% gain over NHS-surfaces irradiated without BSA) (data not shown).

In summary, type, energy and fluence of the incident particles might create Ab surface damages according to Ab surface architecture type.

Resistance of Ab-based surfaces to other space constraints

Considering other space hazards, we observed that loss of surface binding capacities for the tested Ab surfaces under a

Table 3. *Antibody surface stability expressed as % loss in binding capacities after undergoing freeze-drying process, thermal shift and long-time storage*

	NHS-full-length Ab	NHS-Fab	NHS-F(ab′)$_2$	DGL-full-length Ab			DGL-Fab′	Protein A/G-full-length Ab		
				G2	G3	G4				
Binding capacity loss after freeze-drying process (%)	19.2	Nm	25	19.4	6[a]	8.4	NSE[a]	6		
Binding capacity loss after thermal shift (%)	16.0 ± 2.2	NSE	23.0 ± 4.8	13.3 ± 2.8	18.7 ± 2.8	5.2 ± 0.1	ND	9.7 ± 0.4		
Binding capacity loss after storage (period in months)	1–2 NSE	ND	NSE	ND	NSE	ND	20%	NSE		
	3–4 ≤15%		NSE		NSE		ND	≤15%		
	5–6 ≤15%		ND		NSE		ND	≤15%		
	7–8 ≤15%				≤15%			ND		
	9–10 ≤15%				ND			ND		

Mean values were obtained after several analyses (n = 2–7 except if indicated) with four or five replicates. Nm, non-measurable, NSE, non-significant effect, ND, not determined.
[a]Only one freeze drying process was made.

https://doi.org/10.1017/S1473550416000173 Published online by Cambridge University Press

freeze-drying process, thermal shifts and storage never exceed 20% (Table 3) with a slightly better resistance of full-length Ab–DGL-surfaces. Student's *t*-test were used to define if samples were identical or not to their controls (non-lyophilized samples or t_0 for storage) at 95% level of confidence. Results are in the same level than those observed after freeze-drying and long-time storage for Ab grafted by adsorption (de Diego-Castilla *et al.* 2011).

Conclusions

This study highlights the differences in binding capacities between Ab surfaces prepared with full-length or Fab/F(ab′)$_2$ fragments including covalent binding or affinity immobilization in oriented or non-oriented manner. When considering laboratory simulated spatial constraints (irradiation by particles, thermal shifts, freeze-drying and storage), immobilized Ab survived differently according to their initial Ab arrangement to the chip surface (Ab or fragments, oriented/random immobilization, covalent or affinity linkage). As it has been reported in other application fields of Ab surfaces, good accessibilities of active binding sites (for sensitivity of the system), chip stability, low cost and simple method of immobilization should be favoured for efficient analyses. Based on this comment and on our results, we propose that full-length Ab–NHS surfaces with a BSA blocking step (considering cosmic rays constraints) and full-length Ab–DGL(G3/G4) surfaces (considering thermal shifts and freeze-drying constraints) should be preferred in future space missions. To improve the understanding of Ab surfaces resistance to space hazards in real-space constraints with cumulative effects, full-length Ab–NHS surfaces were chosen to be exposed outside the International Space Station on the EXPOSE-R2 platform (Vigier *et al.* 2013; Cottin *et al.* 2014). In recent results (Baqué *et al.* 2015), our group demonstrated that Ab surfaces should have a higher density than the fluence of incident particles in order to minimize the radiation effects on Ab performances. Since DGL(G3/G4) surfaces help to increase the number of immobilized Abs, the Ab–DGL(G3/G4) surfaces could be proposed in future exobiology experiments. Indeed, chip surfaces with high Ab densities would be recommended to better detect differences in the surfaces resistance to real-space constraints (cumulative effects).

Acknowledgements

We would like to thank the French national space agency (CNES) (convention number: 05/2182/00-DCT094) as well as the ANR PCV for financial support (PCV07_186986; D-aminochip). We also thank the Louvain-la-Neuve cyclotron facility staff, Jérôme Caron from the Institut Bergonié staff and the staff from the Laboratori Nazionali del Sud of the Instituto Nazionale di Fisica Nucleare for their help during irradiation experiments. The research leading to these results has received funding from the European Union Seventh Framework Programme FP7/2007-2013 under Grant Agreement no 262010 – ENSAR.

References

Angenendt, P. (2005). Progress in protein and antibody microarray technology. *Drug Discov. Today* **10**(7), 503–511.

Baqué, M., Le Postollec, A., Coussot, G., Moreau, T., Desvignes, I., Incerti, S., Moretto, P., Dobrijevic, M. & Vandenabeele-Trambouze, O. (2011). Biochip for astrobiological applications: investigation of low energy protons effects on antibody performances. *Planet. Space Sci.* **59**(13), 1490–1497.

Baqué, M., Dobrijevic, M., Le Postollec, A., Moreau, T., Faye, C., Vigier, F., Incerti, S., Coussot, G., Caron, J. & Vandenabeele-Trambouze, O. (2015). Irradiation effects on antibody performance in the frame of biochip-based instruments development for space exploration. *Int. J. Astrobiol*. Accepted in September, 2015. doi:10.1017/S1473550415000555

Batalla, P., Fuentes, M., Mateo, C., Grazu, V., Fernandez-Lafuente, R. & Guisan, J.M. (2008). Covalent immobilization of antibodies on finally inert support surfaces through their surface regions having the highest densities in carboxyl groups. *Biomacromolecules* **9**(8), 2230–2236.

Batalla, P., Mateo, C., Grazu, V., Fernandez-Lafuente, R. & Guisan, J.M. (2009). Immobilization of antibodies through the surface regions having the highest density in lysine groups on finally inert support surfaces. *Process Biochem*. **44**, 365–368.

Butler, J.E. (2000). Solid supports in enzyme-linked immunosorbent assay and other solid-phase immunoassays. *Methods* **22**(1), 4–23.

Butler, J.E. (2004). Solid supports in enzyme-linked immunosorbent assay and other solid-phase immunoassays. *Methods Mol. Med*. **94**, 333–372.

Collet, H., Souaid, E., Cottet, H., Deratani, A., Boiteau, L., Dessalces, G., Rossi, J.C., Commeyras, A. & Pascal, R. (2010). An expeditious multigram-scale synthesis of lysine dendrigraft (DGL) polymers by aqueous N-carboxyanhydride polycondensation. *Chemistry* **16**(7), 2309–2316.

Commeyras, A., Collet, H., Souaid, E., Cottet, H., Romestang, B. & Vandenabeele-Trambouze, O. (2006) procede de preparation de polylysines dendrimeres greffes. PCT/FR2006/000952, France.

Cottin, H. *et al*. (2014). Photochemical studies in low Earth orbit for organic compounds related to small bodies, Titan and Mars. Current and future facilities. *Bull. Soc. R. Sci. Liège* **84**, 60–73.

Coussot, G., Perrin, C., Moreau, T., Dobrijevic, M., Postollec, A.L. & Vandenabeele-Trambouze, O. (2011a) A rapid and reversible colorimetric assay for the characterization of aminated solid surfaces. *Anal. Bioanal. Chem*. **399**(3), 1061–1069.

Coussot, G., Faye, C., Ibrahim, A., Ramonda, M., Dobrijevic, M., Postollec, A., Granier, F. & Vandenabeele-Trambouze, O. (2011b) Aminated dendritic surfaces characterization: a rapid and versatile colorimetric assay for estimating the amine density and coating stability. *Anal. Bioanal. Chem*. **399**(6), 2295–2302.

de Diego-Castilla, G., Cruz-Gil, P., Mateo-Martí, E., Fernández-Calvo, P., Rivas, L.A. & Parro, V. (2011). Assessing antibody microarrays for space missions: effect of long-term storage, gamma radiation, and temperature shifts on printed and fluorescently labeled antibodies. *Astrobiology* **11**(8), 759–773.

Dixit, C.K. & Kaushik, A. (2012). Nano-structured arrays for multiplex analyses and Lab-on-a-Chip applications. *Biochem. Biophys. Res. Commun*. **419**(2), 316–320.

Faye, C., Chamieh, J., Moreau, T., Granier, F., Faure, K., Dugas, V., Demesmay, C. & Vandenabeele-Trambouze, O. (2012). *In situ* characterization of antibody grafting on porous monolithic supports. *Anal. Biochem*. **420**(2), 147–154.

Fuentes, M., Mateo, C., Fernández-Lafuente, R. & Guisán, J.M. (2006). Detection of polyclonal antibody against any area of the protein-antigen using immobilized protein-antigens: the critical role of the immobilization protocol. *Biomacromolecules* **7**(2), 540–544.

Gobet, F. *et al*. (2015). Experimental and Monte Carlo absolute characterization of a medical electron beam. *Radiat. Meas* **86**, 16–23. http://dx.doi.org/10.1016/j.radmeas.2016.01.003.

Hassler, D.M. *et al*. (2012). The radiation assessment detector (RAD) investigation. *Space Sci. Rev*. **170**(1), 503–558.

Jonkheijm, P., Weinrich, D., Schröder, H., Niemeyer, C.M. & Waldmann, H. (2008). Chemical strategies for generating protein biochips. *Angew. Chem. Int. Ed. Engl*. **47**(50), 9618–9647.

Jung, Y. *et al*. (2008). Recent advances in immobilization methods of antibodies on solid supports. *Analyst* **133**, 697–701.

Köhler, J. *et al*. (2014). Measurements of the neutron spectrum on the Martian surface with MSL/RAD. *J. Geophys. Res.: Planet*. **119**(3), 594–603.

Kozak, D., Surawski, P., Thoren, K.M., Lu, C.Y., Marcon, L. & Trau, M. (2009). Improving the signal-to-noise performance of molecular diagnostics with PEG-lysine copolymer dendrons. *Biomacromolecules* **10**(2), 360–365.

Le Postollec, A. *et al*. (2007). Development of a Biochip dedicated to planetary exploration. First step: resistance studies to space conditions. In *Journées SF2A 2007 Semaine de l'Astrophysique Française 2007*.

Le Postollec, A. *et al*. (2009a). Monte Carlo simulation of the radiation environment encountered by a biochip during a space mission to mars. *Astrobiology* **9**(3), 311–323.

Le Postollec, A., Coussot, G., Baqué, M., Incerti, S., Desvignes, I., Moretto, P., Dobrijevic, M. & Vandenabeele-Trambouze, O. (2009b) Investigation of neutron radiation effects on polyclonal antibodies (IgG) and fluorescein dye for astrobiological applications. *Astrobiology* **9**(7), 637–645.

Liu, X.H., Wang, H.K., Herron, J.N. & Prestwich, G.D. (2000). Photopatterning of antibodies on biosensors. *Bioconjug. Chem*. **11**(6), 755–761.

Martins, Z. (2011). *In situ* biomarkers and the Life Marker Chip. *Astron. Geophys*. **52**(1), 1.34–1.35.

McKay, C.P. *et al*. (2013). The icebreaker life mission to mars: a search for biomolecular evidence for life. *Astrobiology* **13**(4), 334–353.

McKenna-Lawlor, S., Gonçalves, P., Keating, A., Reitz, G. & Matthiä, D. (2012). Overview of energetic particle hazards during prospective manned missions to Mars. *Planet. Space Sci*. **63–64**, 123–132.

Moreau, T., Faye, C., Baqué, M., Desvignes, I., Coussot, G., Pascal, R. & Vandenabeele-Trambouze, O. (2011). Antibody-based surfaces: rapid characterization using two complementary assays. *Anal. Chim. Acta* **706** (2), 354–360.

O'Neill, P.M. (2010). Badhwar–O'Neill galactic cosmic ray flux model. *IEEE Trans. Nucl. Sci* **57**(6), 3148–3153.

Parro, V., Rivas, L.A. & Gómez-Elvira, J. (2008). Protein microarrays-based strategies for life detection in astrobiology. *Space Sci. Rev*. **135**(2008), 293.

Parro, V. *et al*. (2011). SOLID3: a multiplex antibody microarray-based optical sensor instrument for *in situ* Life detection in planetary exploration. *Astrobiology* **11**(1), 15–28.

Peluso, P. *et al*. (2003). Optimizing antibody immobilization strategies for the construction of protein microarrays. *Anal. Biochem*. **312**(2), 113–124.

Qian, W. *et al*. (2000). Immobilization of antibodies on ultraflat polystyrene surfaces. *Clin. Chem*. **46**(9), 1456–1463.

Romestand, B., Rolland, J.L., Commeyras, A., Coussot, G., Desvignes, I., Pascal, R. & Vandenabeele-Trambouze, O. (2010). Dendrigraft poly-L-lysine: a non-immunogenic synthetic carrier for antibody production. *Biomacromolecules* **11**(5), 1169–1173.

Rusmini, F., Zhong, Z. & Feijen, J. (2007). Protein immobilization strategies for protein biochips. *Biomacromolecules* **8**(6), 1775–1789.

Sims, M.R. *et al*. (2012). Development status of the life marker chip instrument for ExoMars. *Planet. Space Sci*. **72**(1), 129–137.

Singh, P., Moll, F., Lin, S.H., Ferzli, C., Yu, K.S., Koski, R.K., Saul, R.G. & Cronin, P. (1994). Starburst dendrimers: enhanced performance and flexibility for immunoassays. *Clin. Chem*. **40**(9), 1845–1849.

Trevisiol, E., Le Berre-Anton, V., Leclaire, J., Pratviel, G., Caminade, A.M., Majoral, J.P., François, J.M. & Meunier, B. (2003). Dendrislides, dendrichips: a simple chemical functionalization of glass slides with phosphorus dendrimers as an effective means for the preparation of biochips. *New J. Chem*. **27**(12), 1713–1719.

Vigier, F. *et al*. (2013). Preparation of the Biochip experiment on the EXPOSE-R2 mission outside the International Space Station. *Adv. Space Res*. **52**(12), 2168–2179.

Wang, W., Singh, S., Zeng, D.L., King, K. & Nema, S. (2007). Antibody structure, instability, and formulation. *J. Pharm. Sci*. **96**(1), 1–26.

Wängler, C., Moldenhauer, G., Eisenhut, M., Haberkorn, U. & Mier, W. (2008). Antibody-dendrimer conjugates: the number, not the size of the dendrimers, determines the immunoreactivity. *Bioconjug. Chem*. **19**(4), 813–820.

https://doi.org/10.1017/S1473550416000173 Published online by Cambridge University Press